

## Phase Stability and Aging Response of TiC Reinforced Alloy 718

E. F. Wachtel and H. J. Rack

Materials Engineering Program  
Department of Mechanical Engineering  
Clemson University  
Clemson, South Carolina, 29634-0921

### Abstract

The aging kinetics and precipitation reactions of an alloy 718 matrix composite were analyzed and compared to ingot and P/M alloy 718 material. The techniques employed in this study included isothermal aging, hardness testing, differential scanning calorimetry, Scanning and transmission electron microscopy and energy dispersive X-ray spectroscopy. It was found that the aging kinetics of the composite were generally faster and that the precipitation sequence is different than that of conventional alloy 718. The differences in kinetics and precipitation sequence are attributed to the reaction between the matrix and the reinforcing phase. The Titanium carbide reacts with the matrix Niobium forming a mixed MC carbide, this results in a matrix depleted of niobium and enriched in titanium.

## INTRODUCTION

Metal matrix composites (MMC's) are being developed to improve specific stiffness ( $E/\rho$ ), specific strength ( $\sigma/\rho$ ) and high temperature performance. They are intended to combine the high toughness and ductility of a metal matrix with the high strength and stiffness of a ceramic reinforcing phase. While properties of discontinuously reinforced MMC's typically fall short of the values predicted by the Rule of Mixtures, substantial property improvements can still be made. While most previous efforts have involved an aluminum, titanium or magnesium matrix, recent advances in material processing technology have resulted in the development of an intermediate temperature MMC based on a matrix of Alloy 718.

The precipitation reactions in alloy 718 have been studied extensively. The precipitation sequence is shown in Table 1 and the time-temperature-transformation curve (TTT) is depicted in Figure 1. The  $\gamma'$  phase is a disc or cuboidal shaped, coherent precipitate with an ordered FCC structure ( $L1_2$ ) having a stoichiometry based on the  $Ni_3Al$  composition, with Ti freely substituting for Al.  $\gamma''$  is a metastable, lens shaped, coherent precipitate with an ordered body centered tetragonal crystal structure ( $D0_{22}$ ) having a stoichiometry based on  $Ni_3Nb$ . Ti and possibly Al can substitute for the Nb.  $\delta$  is a stable, plate-like, incoherent precipitate with an orthorhombic structure ( $D0_a$ ), having a stoichiometry based on  $Ni_3Nb$ . Studies on material produced using a powder metallurgy (P/M) processing approach have shown that the precipitation reactions are similar to those of the conventional products (13,14).

Table I. Precipitation Reactions In Alloy 718

## **PRECIPITATION REACTIONS IN ALLOY 718**

$\gamma$	$\Rightarrow$	$\gamma'$	$\Rightarrow$	$\gamma''$	$\Rightarrow$	$\delta$
FCC		FCC		BCT		ORTHORHOMBIC
		$L1_2$		$D0_{22}$		$D0_a$ ( $Cu_3Ti$ )
		CUBOIDAL		LENS SHAPED		PLATELET
$a = 0.359nm$		$a = 0.362nm$		$a = 0.362nm$		$a = 0.514nm$
				$b = 0.741nm$		$b = 0.425nm$
						$c = 0.453nm$

Various carbides are present in the alloy 718 system including: an MC type (usually Ti or Nb carbide or carbo-nitride) with a blocky morphology and a B<sub>1</sub> structure, an M<sub>6</sub>C type, which is derived from the decomposition of MC and which typically has a blocky, grain boundary morphology, a Cr<sub>7</sub>C<sub>3</sub> type which has a blocky intergranular morphology and a M<sub>23</sub>C<sub>6</sub> type which forms from the decomposition of either MC or Cr<sub>7</sub>C<sub>3</sub> and has a grain boundary platelet morphology. In addition to  $\gamma''$  strengthening, investigators have suggested that Niobium carbide (NbC) precipitation may also enhance the properties of alloy 718 (1,2,5,7,8,9,15). Carbide type, distribution and morphology have been shown to affect properties, particularly ductility and stress rupture (15). Finally, it is reported that the solubility of carbon in alloy 718 increases substantially at temperatures above 980°C (15).

Previous experience with aluminum and magnesium matrix composites has shown that the aging kinetics and precipitation reactions may be altered by the presence of a reinforcing phase (16-19). This phenomenon is particularly pronounced in systems where the precipitation reactions exhibit heterogeneous nucleation. Heterogeneous nucleation is enhanced due to a minimization of the distortional free energy associated with a dislocation network. In addition, the growth of precipitates is enhanced by dislocation pipe diffusion. One possible cause of a dislocation network is thermal strain associated with the mismatch in coefficient of thermal expansion between the matrix and the reinforcement. Dislocation densities on the order of 10E13/cm<sup>2</sup> have been reported at the matrix reinforcement interface (20).

It is well established that the  $\gamma'$  phase nucleates heterogeneously in alloy 718, typically at extrinsic stacking faults or at intrinsic slip dislocation (4,21,22).  $\gamma''$  nucleation is

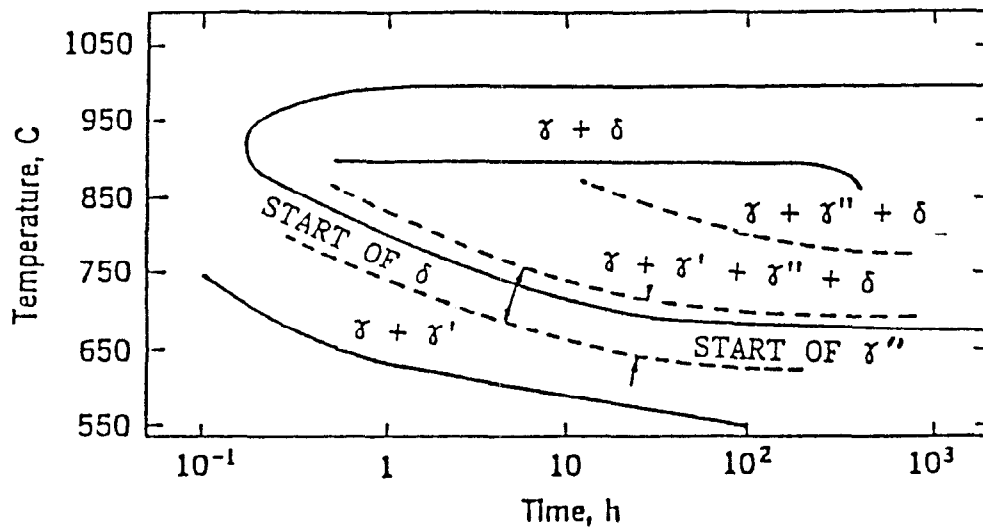


Figure 1. TTT diigram of alloy 718. Ref 10.

reported to be intimately associated with existing  $\gamma'$  precipitates (7). In addition, NbC is reported to nucleate heterogeneously (1,2,7,23). Based on the above considerations, it would be anticipated that the aging kinetics of alloy 718 would be affected by the addition of a ceramic reinforcing phase.

The primary objective of this study is to determine the effect of a reinforcing phase addition on the precipitation reactions and aging kinetics of an alloy 718 matrix composite. The secondary objective is to study the stability of TiC as a reinforcing phase in nickel base superalloy MMC's.

#### EXPERIMENTAL PROCEDURES

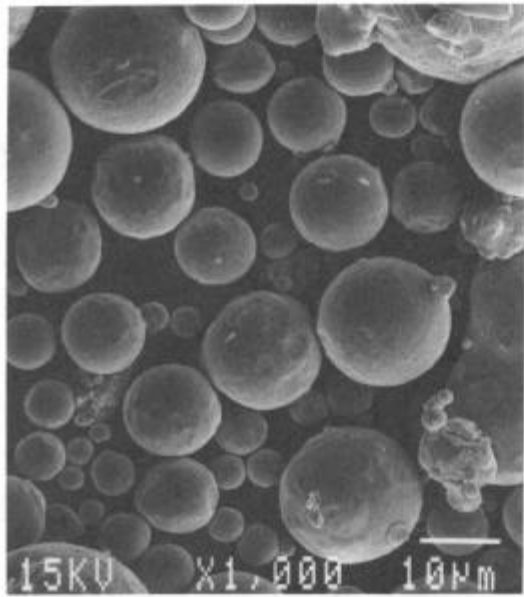
The materials used in this study were as follows: a P/M composite of alloy 718 with a 20 volume percent addition of TiC, P/M 718 and ingot 718. The composition of the ingot and the powder are shown in Table 2. It can be seen that the composition of the ingot and the powder are almost identical in every respect, thereby eliminating the effect of compositional variation on the aging response. The composite and the P/M material were produced by DWA Composite Specialists. Gas atomized powder with a -200 mesh size was supplied by Carpenter Technology, INC, Figure 2(a). The reinforcing phase for the composite was TiC, Figure 2(b). The P/M materials were wet blended, dried, canned in mild steel and evacuated. Compaction of the material was achieved by hot isostatic pressing at 1150°C for three hours at a pressure of 15 KSI, with subsequent extrusion being carried out at 1040°C with an extrusion ratio of 19:1. In order to eliminate the effect of thermo-mechanical processing history on the aging response, the ingot material was subjected to the same processing sequence.

Table II. Chemical Composition of Ingot and Powder Material

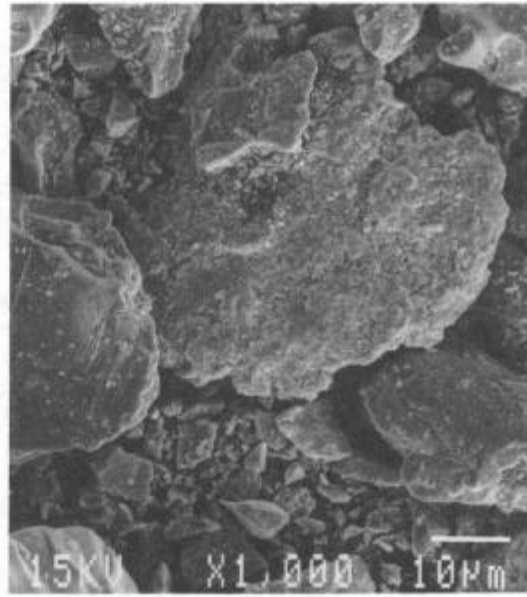
Element	Ni	Fe	Cr	Mo	Ti	Al	Nb	Mn	Si
Powder	52.81	18.28	18.38	3.08	.99	.61	5.31	.12	.16
Ingot	52.52	18.67	18.29	3.07	.97	.59	5.37	.09	.10

The microstructure of the composite material was evaluated using a JEOL JSM IC848 scanning electron microscope in the backscatter mode. Backscatter SEM provides Z number contrast, which allows identification of phases with different composition. Semi-quantitative analysis of the various phases present in the backscatter micrographs was done using energy dispersive X-ray spectroscopy (EDS) in the spot mode (beam spot diameter of .02  $\mu\text{m}$ ), the system being calibrated using a copper standard.

The aging kinetics of the three materials were examined through isothermal aging studies. The hardness of solution treated and quenched samples was measured as a function of isothermal aging time for a variety of aging temperatures. These studies were carried out utilizing temperatures varying from 650°C to 870°C with times ranging from 0.5 to 1000 hours.



(a)



(b)

Figure 2. SEM micrograph of a) 718 powder and b) titanium carbide powder.

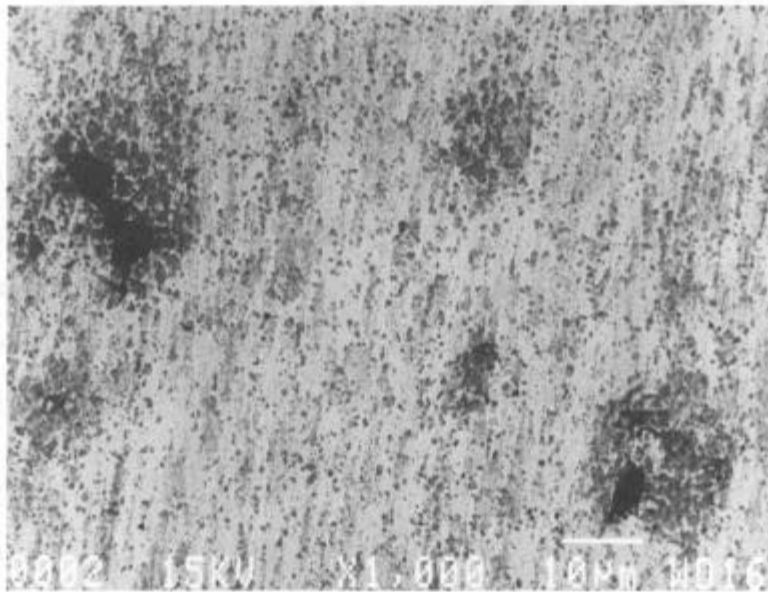


Figure 3. Backscatter SEM micrograph of as solution treated composite.

In addition, differential scanning calorimetry was used to compare the P/M material to the composite.

Thin foil transmission electron microscopy studies were conducted to determine the location and nature of the precipitate reactions and the type and extent of the matrix/reinforcing phase interfacial reaction. Precipitates and reaction products were analyzed using selected area electron diffraction (SAED) and energy dispersive spectroscopy (EDS).

## RESULTS AND DISCUSSION

Figure 3 shows typical SEM backscatter electron micrographs of the 1150°C solution treated composite. Three distinct phases are obvious in these micrographs. Using the EDS capability of the microscope in the spot mode, the three phases have been identified. The spectrum for the black phase (TiC) is shown in Figure 4. In general, the TiC was evenly distributed throughout the matrix. The volume fraction of the reinforcing phase and the size of the particulate were much smaller than anticipated. The average volume fraction of particulate was on the order of five percent (5%) and the particulate size ranged from 5 to 10 microns. The spectrum for the gray phase is shown in Figure 5. This phase appears to be a mixed carbide of Ti and Nb, probably a mixed MC type carbide. This is reasonable since both carbides have the same structure  $B_1$  and are completely soluble in one another with Ti and Nb occupying various sites on a carbon sublattice. In some cases, the TiC is surrounded by the mixed MC carbide. This is due to competition between Ti and Nb at the reinforcement interface, resulting in the formation of the mixed carbide, depletion of the matrix Nb and an increase in the matrix Ti content. Finally, the spectrum for the light phase is shown in Figure 6. This is the matrix, alloy 718.

Preliminary results of the DSC scans are shown in Figure 7. The DSC results indicate differences in the precipitation reactions between the two systems. The scan of the P/M material shows three main peaks. The sharp peak at 810°C is believed to be due to precipitation of the  $\delta$  phase. The broad peak from 550 - 650°C is believed to be due to a combination of gamma prime and gamma double prime precipitation. The diffuse peak from 300 - 400°C is most likely due to carbide precipitation. The scan of the composite material has four distinct peaks. The peak at 1000°C is believed to be due to dissolution and or decomposition of the carbides. The peak at 690°C is due to the precipitation of the eta phase, while the peak at 550°C has been attributed to the gamma prime phase. The broad peak from 300- 400°C is due to carbide precipitation. The differential scanning calorimetry experiments are continuing, 100 hour isothermal scans are planned for temperatures ranging from 400 °C to 1100 °C to reevaluate the TTT diagram.

The results of the aging studies are shown in Figure 8. It is apparent from the results that the aging kinetics of the composite vary considerably from the aging kinetics of the unreinforced material. At aging temperatures below 815°C, the aging kinetics of the composite are substantially faster than

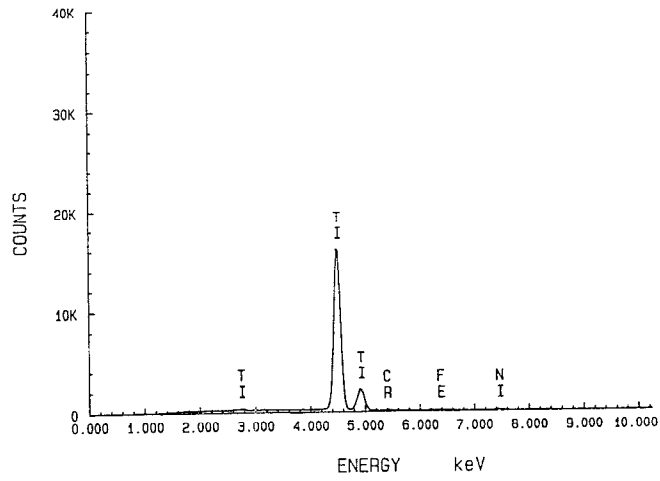


Figure 4. EDS spectrum of titanium carbide.

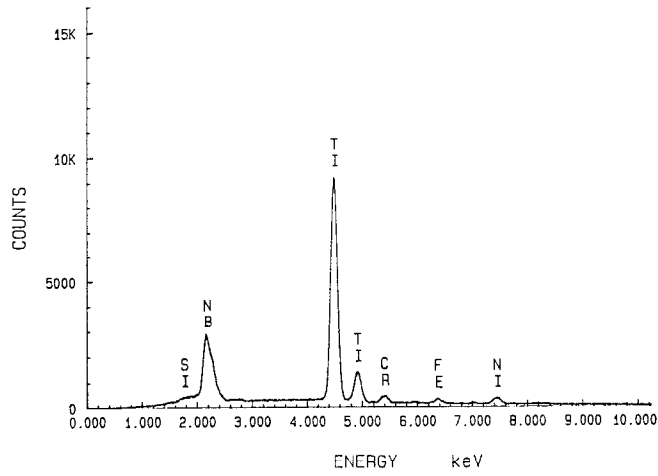


Figure 5. EDS spectrum of mixed MC Carbide.

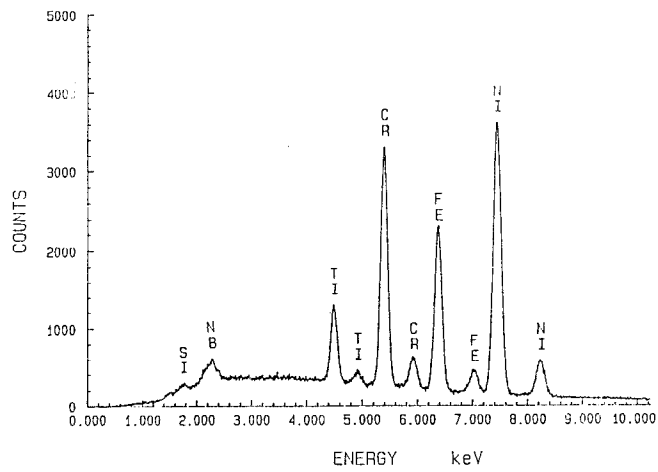
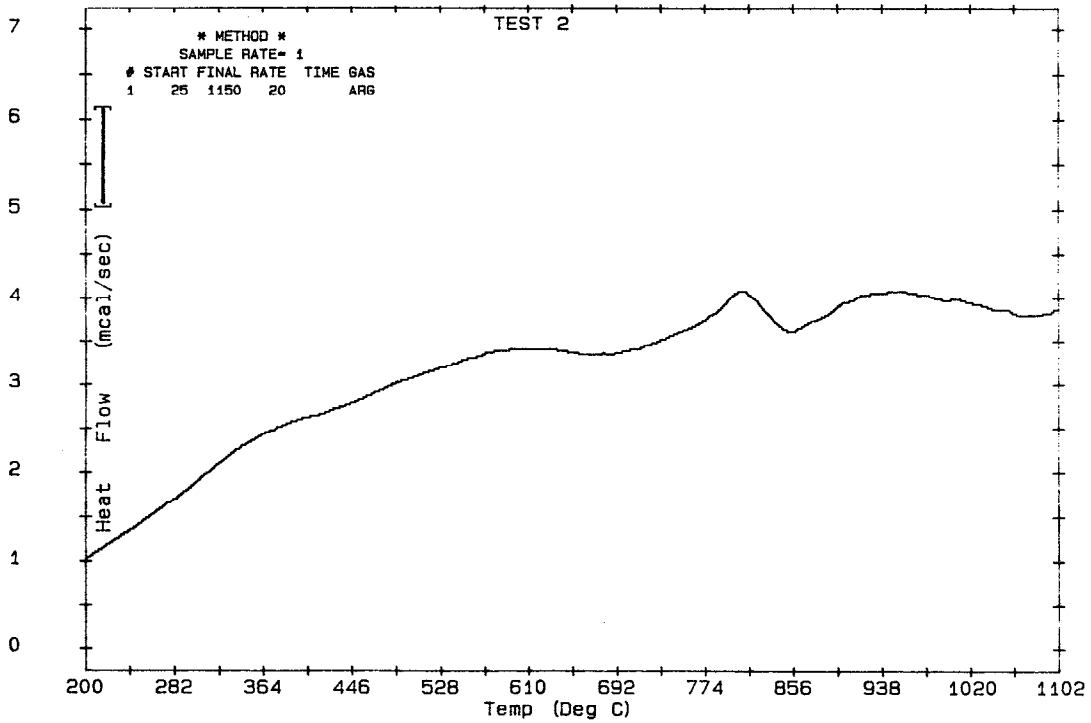
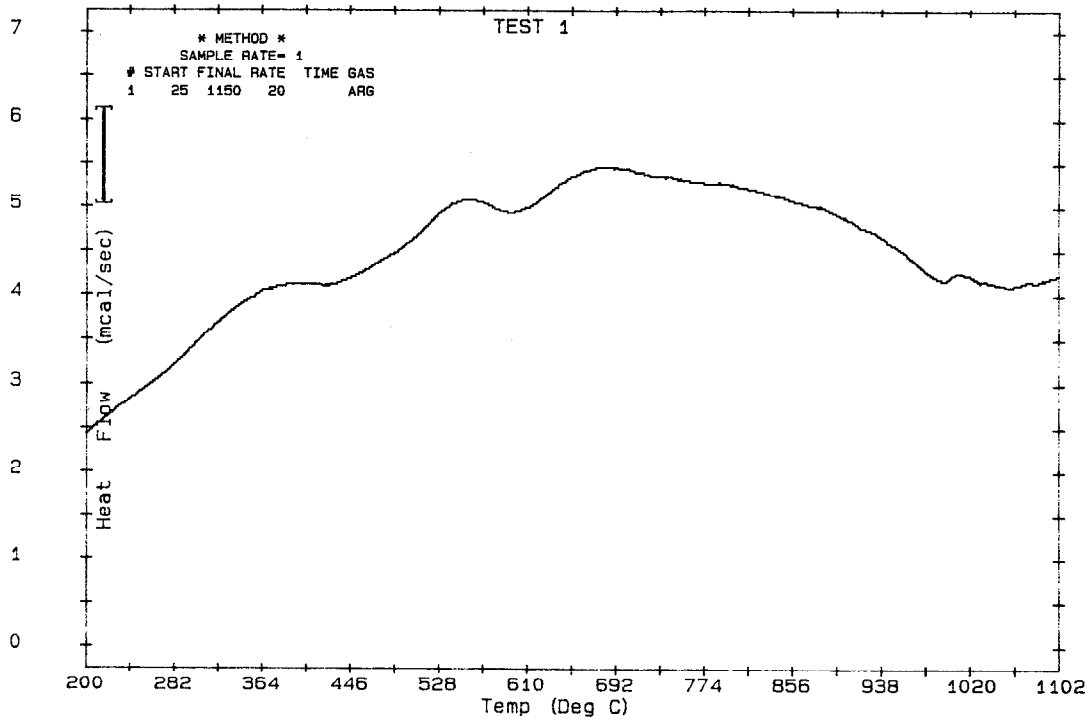


Figure 6. EDS spectrum of matrix, alloy 718.



(a)



(b)

Figure 7. Differential scanning calorimetry scans of a) alloy 718 and b) composite material.



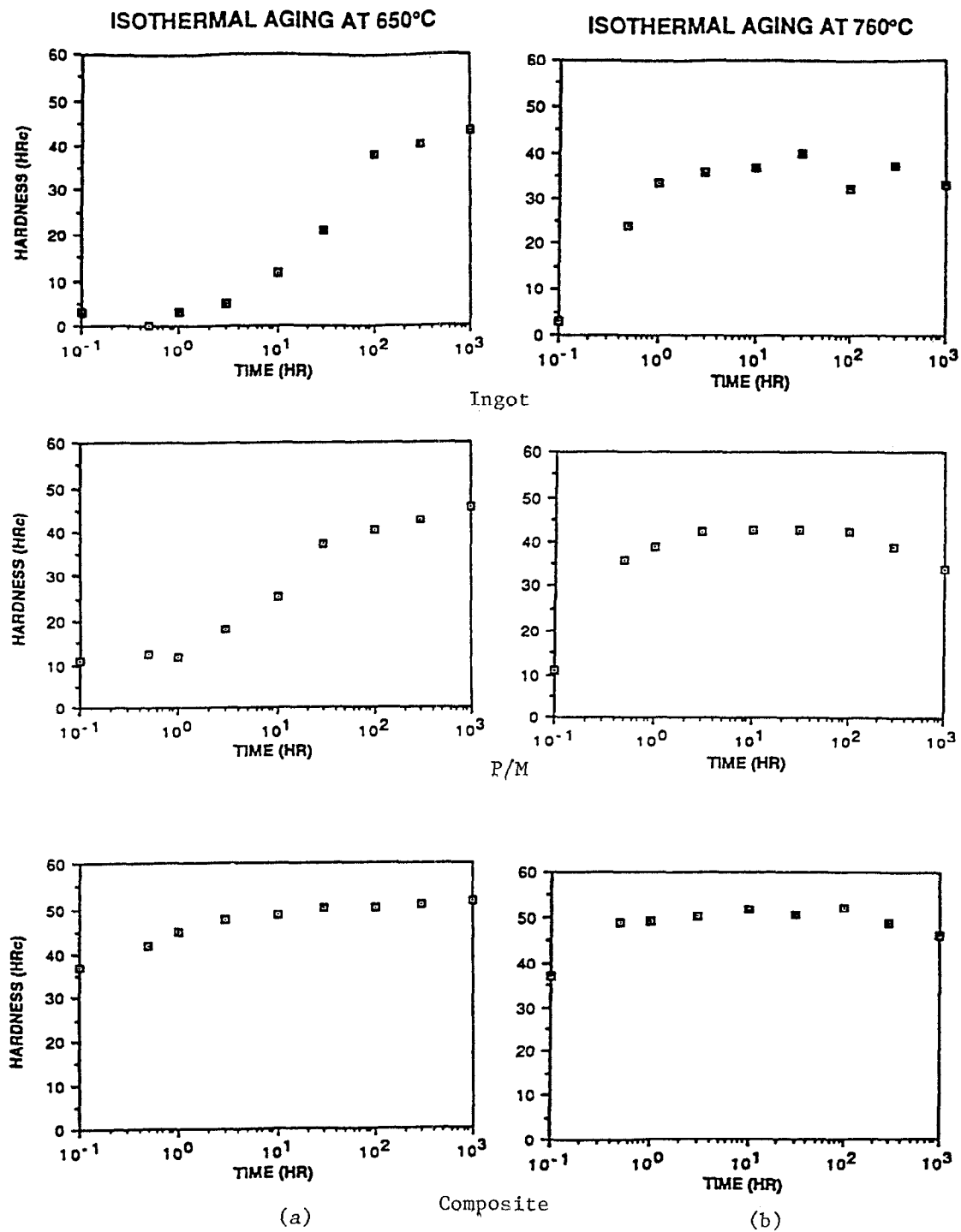
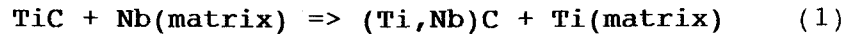


Figure 8. Isothermal aging response for ingot, P/M and composite material at a) 650 C and b) 760 C.

those of the unreinforced material. At temperatures of 815°C and above, the kinetics of both are similar, with overaging occurring in less than 0.5 hours.

It is hypothesized that the acceleration of the aging kinetics in the composite system is based on the reaction shown in equation 1.



During elevated temperature thermo-mechanical processes, some of the reinforcing phase goes into solution. On cooling, Nb tends to compete with Ti at the matrix/precipitate interface resulting in the formation of mixed MC carbides and a matrix which has been enriched in Ti and depleted of Nb.

TEM studies have confirmed this hypothesis, precipitates of (Ti,Nb)C have been detected in the composite material at all temperatures, a typical TEM micrograph and EDS spectra are shown in Figure 9. These results confirm the earlier EDS work on the SEM but indicated that the actual Nb concentration of the precipitates is as high as 40%.

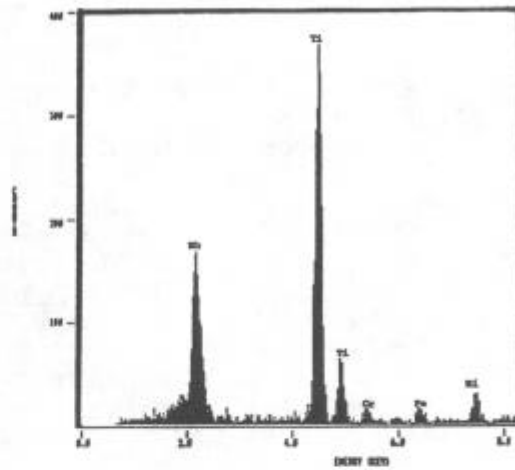
Increases in Ti content has been shown to accelerate the formation of  $\gamma'$  precipitates (10, 23,28). In addition, increased matrix Ti content could promote the formation of the  $\eta$  phase ( $\text{Ni}_3\text{Ti}$ ) which is not normally observed in alloy 718, but which has been reported in nickel base superalloys having high Ti contents (10). Eta phase has been detected in the composite material at both the 815 and 870°C aging temperatures, as shown in Figure 10. In addition, matrix Ti content was much higher in the composite material.

#### CONCLUSIONS

1. The the aging kinetics (rate of reaction) of the composite material is substantially different than that of the unreinforced materials, while the ingot and the P/M material are similar at all temperatures.
2. The matrix and reinforcement react to form a mixed MC carbide (Ti/Nb)C. This reaction alters the matrix chemistry, depleting the Nb concentration and increasing the Ti concentration. As a result of the modification in matrix chemistry, the precipitation kinetics and reaction sequence is altered. The increased Ti concentration results in accelerated  $\gamma'$ coarsening and the precipitation of the eta phase.



(a)



(b)

Figure 9. TEM micrograph of as solution treated composite and b) EDS spectrum of carbide particle.

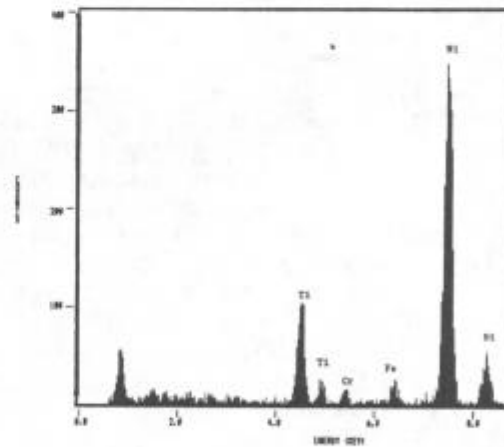
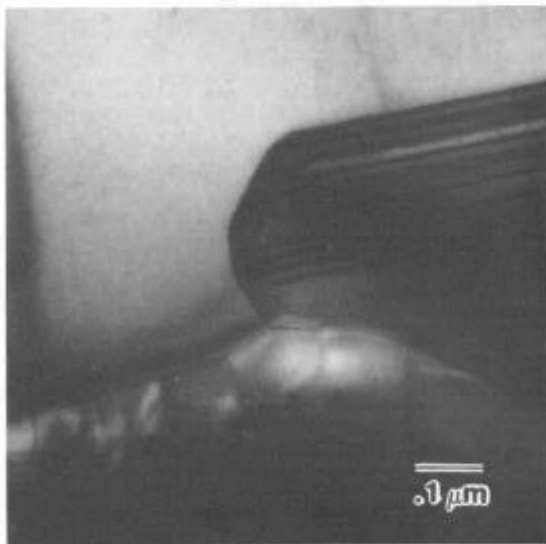


Figure 10. TEM micrograph of composite material aged at 870 C for 300 hours, showing eta precipitate and carbide particle and b) EDS spectrum of the eta precipitate.

## REFERENCES

1. H. L. Eiselstein, ASTM STP 369, Philadelphia, 1965, 62-79.
2. M. Kaufman and A. E. Palty, Trans. of the Met. Society of AIME 221, 1253-1261 (1961).
3. J. F. Barker, E. W. Ross and J. F. Radavich, J. of Metals 22, 31-41, (1970).
4. R. S. Cremisio, J. F. Radavich and H. M. Butler, Int. Symp. on Structural Stability in Superalloys, Seven Springs, PA, 1968, 597-618.
5. W. J. Boesch and H. B. Canada, Ibid
6. D. F. Paulonis, J. M. Oblak and D. S. Duvall, Trans. of the ASM 62, 611 - 622 (1969).
7. R. Cozar and A. Pineau, Met. Trans. 4, 47-59 (1973).
8. J. W. Brooks and P. J. Bridges, High Temperature Alloys for Gas Turbines and Other Applications 1986, ed. W. Betz, et al., D. Reidel Publishing Co., Dordrecht, Holland, 1968, 1431-1440.
9. J. F. Barker, D. D. Kruger and D. R. Chang, Advanced High-Temperature Alloys: Processing and Properties, ed. S. Allen, R. M. Pelloux and R. Witmer, ASM, Metals Park, Ohio, 1986, 125-137.
10. R. F. Decker, Steel Strengthening Mechanisms Symposium, Zurich, Switzerland, May 1969, 147-170.
11. E. A. Fell, Metallurgia 63, 157-166, (1961).
12. J. M. Oblak, W. A. Owczarski and B. H. Kear, Acta Met., 19, 355-363, (1971).
13. H. F. Merrick, Met. Trans. 7A, 505-514 (1976).
14. K. Hajmrle, R. Angers and G. Dufour, Met. Trans. 13A, 5-12
15. E. L. Raymond, Trans. of the Met. Society of AIME 239, 1415-1422 (1967).
16. H. J. Rack and J. W. Mullins, High Strength Powder Metallurgy Aluminum Alloys II, ed. G. J. Hildeman and M. J. Koczak, AIME, 1986, 155-171.
17. H. J. Rack, Dispersion Strengthened Aluminum Alloys, ed. Y-W. Kim, The Met. Society, Warrendale, PA, 1988, in press.
18. H. J. Rack and R. W. Krenzer, Met. Trans. 8A, 335-346
19. H. J. Rack, Mat. Sci. and Eng., 29, 179-188 (1977)
20. M. Vogelsang, R. J. Arsenault and R. M. Fisher, Met. Trans., 17A, (1986) 379-389
21. A.A. Guimaraes and J.J. Jonas, Met. Trans. 12A, 1655- 1666,
22. D. D. Krueger, S. D. Antolovich and R. H. Van Stone, Met. Trans. 18A, 1431-1449, (1987).
23. F. J. Rizzo and J. D. Buzzanell, Int. Symp. on Structural Stability in Superalloys, Seven Springs, PA, 1968, 501-543.
24. ASM Metals Handbook; 9th Edition, Volume 3, ASM, Metals Park, Ohio, 1980.
25. Areospace Structural Metals Handbok, Metals and Ceramics Information center, Battelle Columbus division.
26. E. Supan, DWA Composite Specialists, Unpublished Data.
27. P. S. Kotval, Trans. Met. Society of AIME, Vol. 242, 1764-5, (1968)
28. J. P. Collier, S. H. Wong, J. C. Phillips and J. K. Tien, Met. Trans., Vol. 19A, 1657-1666, (1988).
29. M. Sundararaman, P. Mukhopadhyay and S. Banerjee, Met. Trans., Vol. 19A, 453-465, (1988).
30. M. J. Donachie and O. H. Kriege, J. of Materials, JMLSA, Vol.7 (3), 269-278, (1972).